# Harnessing Chemical Raman Enhancement for Understanding Organic Adsorbate Binding on Metal Surfaces

Alexey T. Zayak,[†] Hyuck Choo,[‡] Ying S. Hu,[¶] Daniel J. Gargas,[†] Stefano Cabrini,[†] Jeffrey Bokor,[§] P. James Schuck,[*,†] and Jeffrey B. Neaton[*,†]

*Molecular Foundry, Lawrence Berkeley National Laboratory, Berkeley CA 94720, USA, The Moore Laboratory, Electrical Engineering, California Institute of Technology, Pasadena, CA 91125, USA, Waitt Advanced Biophotonics Center, Salk Institute, La Jolla, CA 92037, USA, and Department of Electrical Engineering and Computer Sciences, UC Berkeley, Berkeley CA 94720-1770, USA*

E-mail: PJSchuck@lbl.gov; JBNeaton@lbl.gov

[*]To whom correspondence should be addressed
[†]Molecular Foundry, LBNL
[‡]California Institute of Technology
[¶]Waitt Advanced Biophotonics Center
[§]University of California at Berkeley

**Abstract**

Surface enhanced Raman spectroscopy (SERS) is a known approach for nanoscale molecule detection. While SERS measurements have focused on enhancing the signal for sensing trace amounts of a chemical moiety, understanding how the substrate alters molecular Raman spectra can enable optical probing of analyte binding chemistry. Here, we examine binding of trans-1,2-two(4-pyridyl) ethylene (BPE) to Au surfaces, and understand variations in experimental data that arise from differences in how the molecule binds to the substrate. Monitoring differences in the SERS as a function of incubation time, a period of several hours in our case, reveals that the number of BPE molecules that chemically binds with the Au substrate increases with time. In addition, we introduce a direct method of accessing relative chemical enhancement from experiments that is in quantitative agreement with theory. The ability to optically probe specific detailes of metal/molecule interfaces opens up possibilities for using SERS in chemical analysis.

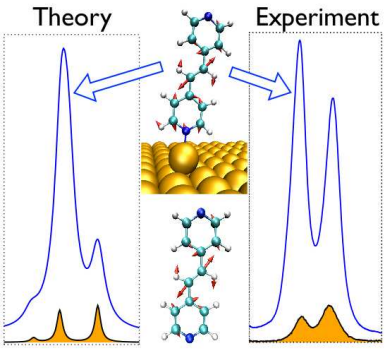


**Keywords:**

Raman spectroscopy, SERS, Chemical enhancement, Density Functional Theory, metal-organic interface

While the Raman scattering from a typical single molecule is many orders of magnitude below detection limits, cross sections can be deliberately enhanced by factors greater than $10^8$ for molecules deposited near metal nanostructures or on rough metal substrates by conversion of incident light into surface plasmons.[1–6] This effect is known as surface enhanced Raman spectroscopy (SERS). While the majority of the enhancement in SERS originates with the large local electromagnetic field and optical density of states experienced by the adsorbate molecules associated with the roughened surface, chemical interactions between the adsorbate molecules and the metal substrate can also alter the Raman signal and contribute to the effect frequently referred to as "chemical enhancement" (CE).[4,7] CE can result in pronounced changes in relative peak intensities,[8] significantly different from gas- or solution phase spectra , which are directly connected with the local chemical environment of the reporting molecules.

Recent theoretical studies[9–16] have led to new quantitative insight into how metal-molecule binding influences SERS data, in large part rationalizing CE in terms of the interfacial electronic structure energy level alignment between frontier molecular orbital energy and the metal Fermi energy, which sets the scale of the overall mode-independent multiplicative factor,[17] and the mode-specific degree to which a particular vibrational mode alters the interfacial energy level alignment.[8]

In this article, we use chemical contributions to SERS, computed with a parameter-free theory and measured experimentally, to understand how trans-1,2-two(4-pyridyl) ethylene (BPE), a frequently-used model system in SERS studies, binds to a Au SERS substrate. Utilizing incubation time dependent variations in our SERS data for BPE we are able to extract relative CE from experimental data. Comparing directly to DFT calculations, we explain controversial spectral variations in past experimental data for BPE in the literature. We further introduce a new experimental analysis to account for the unknown numbers of bound and unbound molecules, allowing quantitative correspondence with the theory. We find that the ratio of two peak intensities in BPE's SERS spectra are extremely sensitive to whether BPE is chemically bound to Au or not; moreover, if bound, then peak intensities can provide quantitative information on how BPE is bound. From a comparison of calculated binding geometries of BPE on Au to experiment, we find a clear trend

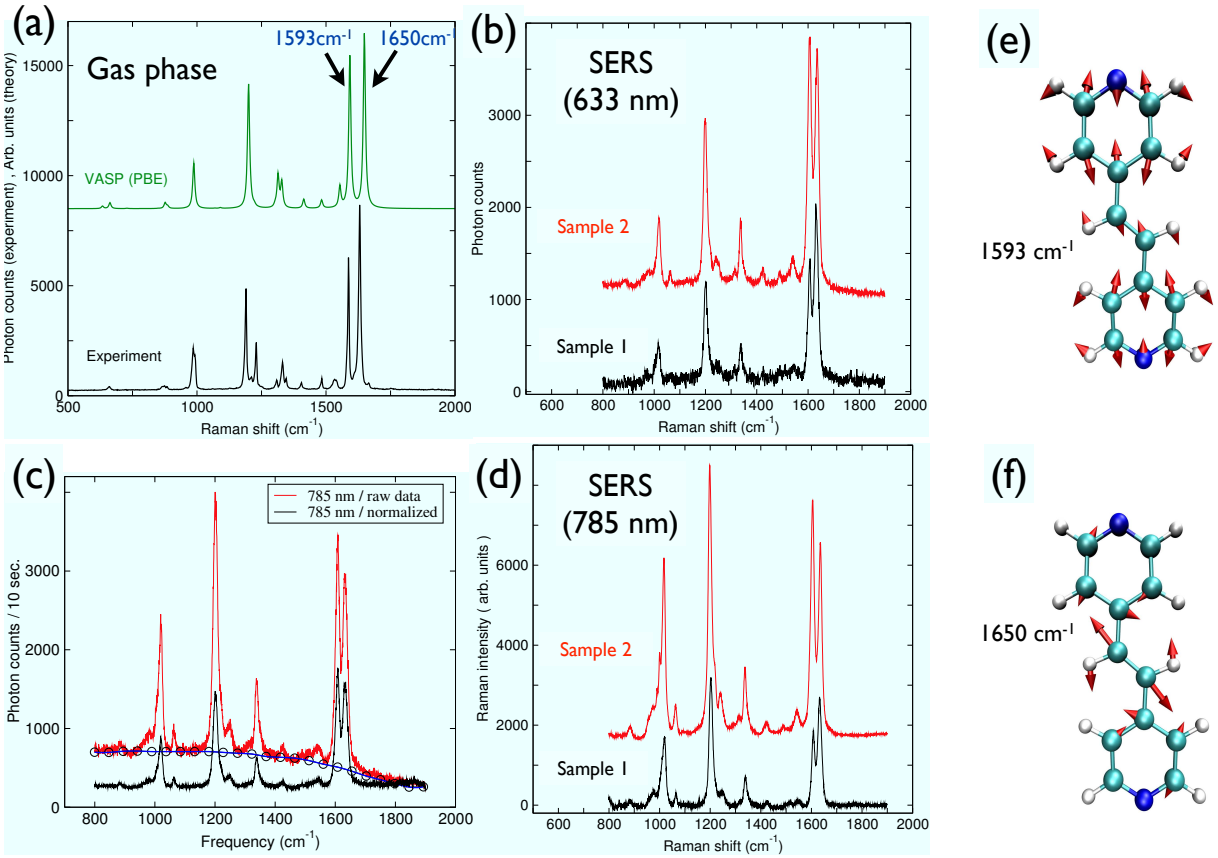


Figure 1: (a) Calculated gas-phase and measured (from purified crystalline powder) Raman spectra of BPE. In Figure S1, we show displacement patterns for the corresponding Raman active modes of BPE. (b) SERS spectra of BPE measured from two different samples (Sample 1 was incubated for 1 hour; Sample 2 was incubated for 1 day), using an excitation wavelength 632.8 nm. The two samples show prominent differences in relative intensities of 1593 $cm^{-1}$ and 1650 $cm^{-1}$ peaks. (c) Spectra showing the effect of using the fluorescence background as a scaling factor renormalizing the nonuniform EM enhancement (plasmon dispersion correction) in 785 nm data. Blue circles show the plasmonic background of the raw spectrum (shown in red). We divide the red spectrum by the corresponding background profile shown with the blue circles, yielding the black spectrum. The latter becomes similar to the 633 nm spectrum shown in panel (b). (d) The same as (b) using 785 nm excitation wavelength. (e,f) Vibrational modes corresponding to the Raman peaks at 1593 $cm^{-1}$ and 1650 $cm^{-1}$.

suggesting that on rough Au surfaces BPE binds to Au atoms with higher nearest neighbor coordination. With a quantitative understanding of non-resonant contributions to CE from first-principles calculations, we can extract detailed information about surface chemistry.

In our experiments, SERS substrates consisting of roughened SiGe surfaces coated with 30 nm of Au are incubated in 50 micromolar BPE solution (Sigma Aldrich W361607) in methanol, then

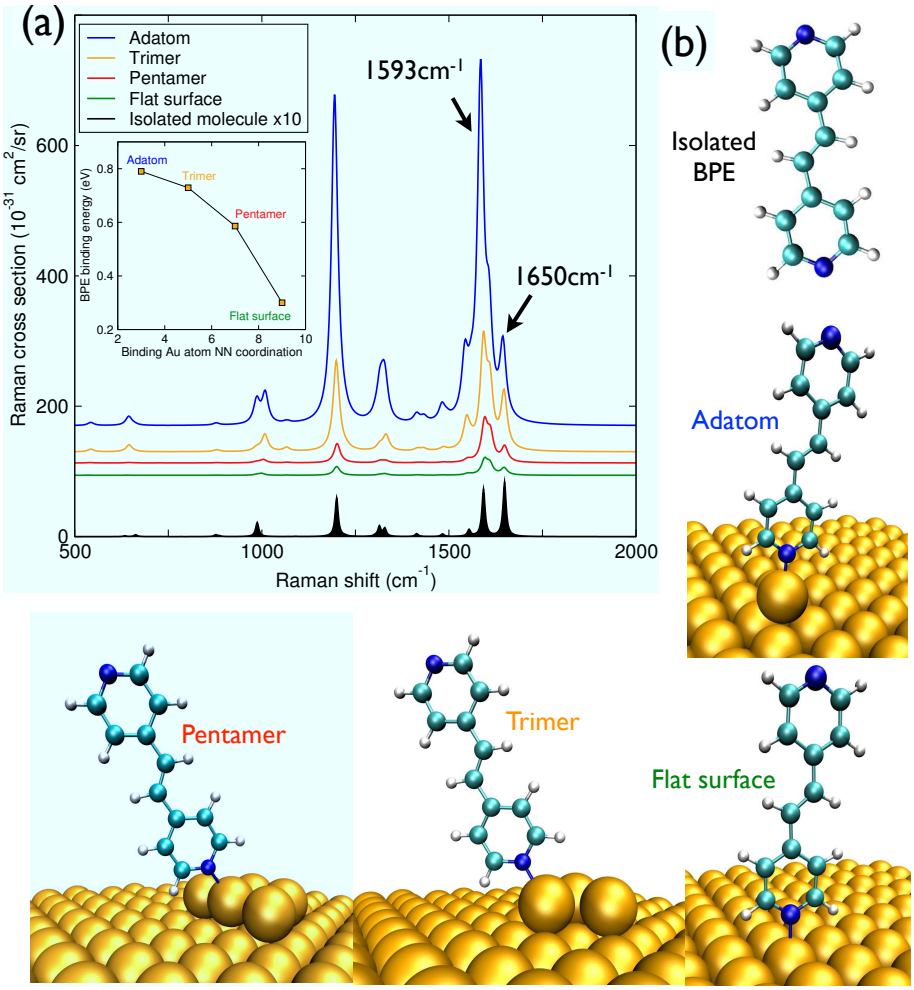


Figure 2: (a) Calculated Raman spectra for isolated BPE (bottom spectrum) and BPE adsorbed on four different binding sites: Adatom, Trimer, Pentamer, Flat Surface. (b) Fully relaxed binding geometries for BPE on (111) gold surface. The binding geometries differ in the nearest neighbor coordination numbers for binding Au atom. Panel (a) and the inset in it show that the binding energies as well the overall Raman intensity depend on the binding site coordination number.

gently rinsed with methanol and dried by nitrogen gas. The 50 uM concentration was determined to be low enough to observe slow ( in the range of hours ) binding kinetics of BPE. A 1 mM concentration, as used previously,[18] led to much faster ( few minutes ) binding of BPE, and was not suitable for the purpose of this study. Raman (neat solution) and SERS spectra are collected at two wavelengths, 632.8 nm and 785 nm, using an inverted microscope set-up coupled to a spectrometer (Acton SpectraPro 2300i) equipped with a liquid-nitrogen-cooled charge-coupled device (CCD) camera.

In Figure Figure 1, we summarize the results of our measurements. The Raman spectra exhibit several prominent peaks, but two modes have particularly strong intensities at 1593 $cm^{-1}$ and 1650 $cm^{-1}$ (Fig. Figure 1(a)), with the 1650 $cm^{-1}$ peak consistently about 10% higher than 1593 $cm^{-1}$ in solution. However, when BPE is deposited on a SERS substrate, we measure varied peak intensities ratios. Figure Figure 1(b) shows SERS data collected from two different samples ( 1 and 2 ), taken at an excitation wavelength of 633 nm. Figure Figure 1(d) shows data from the same samples, using a 785 nm excitation wavelength. Independent of excitation wavelengths, samples 1 and 2 show different relative intensities of the two peaks at 1593 $cm^{-1}$ and 1650 $cm^{-1}$. This is consistent with prior variations in experimental data, with some experiments reporting $I(1593) > I(1650)$,[19–21] while others reporting the opposite.[22–24] Although, direct comparisons between prior experiments can be difficult due to differing solution concentrations and substrate conditions, the only difference between samples 1 and 2 in our experiments is the length of incubation time: 1 hour and 1 day for samples 1 and 2, respectively.

We note that the substrate-induced enhancement is not uniform and if we neglect the frequency dependence of the plasmon resonances, the peak intensity at 1200 $cm^{-1}$, for example, is much greater for measurements taken at 785 nm than at 633 nm Figure 1(b,d). Using the fluorescence background to renormalize both spectra, a so-called plasmon dispersion correction,[25,26] as shown in Figure 1(c), brings the 785 nm and 633 nm spectra in agreement. But because the 1593 $cm^{-1}$ and 1650 $cm^{-1}$ peaks are so close in wavenumber, the plasmon dispersion correction does not appreciably change the intensity variations between them: as the EM enhancement does not vary on the scale of 100 $cm^{-1}$, it is not responsible for variations between 1593 $cm^{-1}$ and 1650 $cm^{-1}$ peaks, both here and elsewhere.[19–24] We also note that to account for any influence of possible blinking, our measurements are averaged over time.

To understand these data, we turn to DFT calculations, and focus on chemical enhancement, using the Vienna Ab-initio Simulations Package (VASP) and a generalized gradient approximation.[27,28] To model BPE on Au(111), we consider binding sites on a periodic Au(111) slab consisting of 5 atomic layers of Au stacked along [111] with 16 atoms per layer, in a supercell with

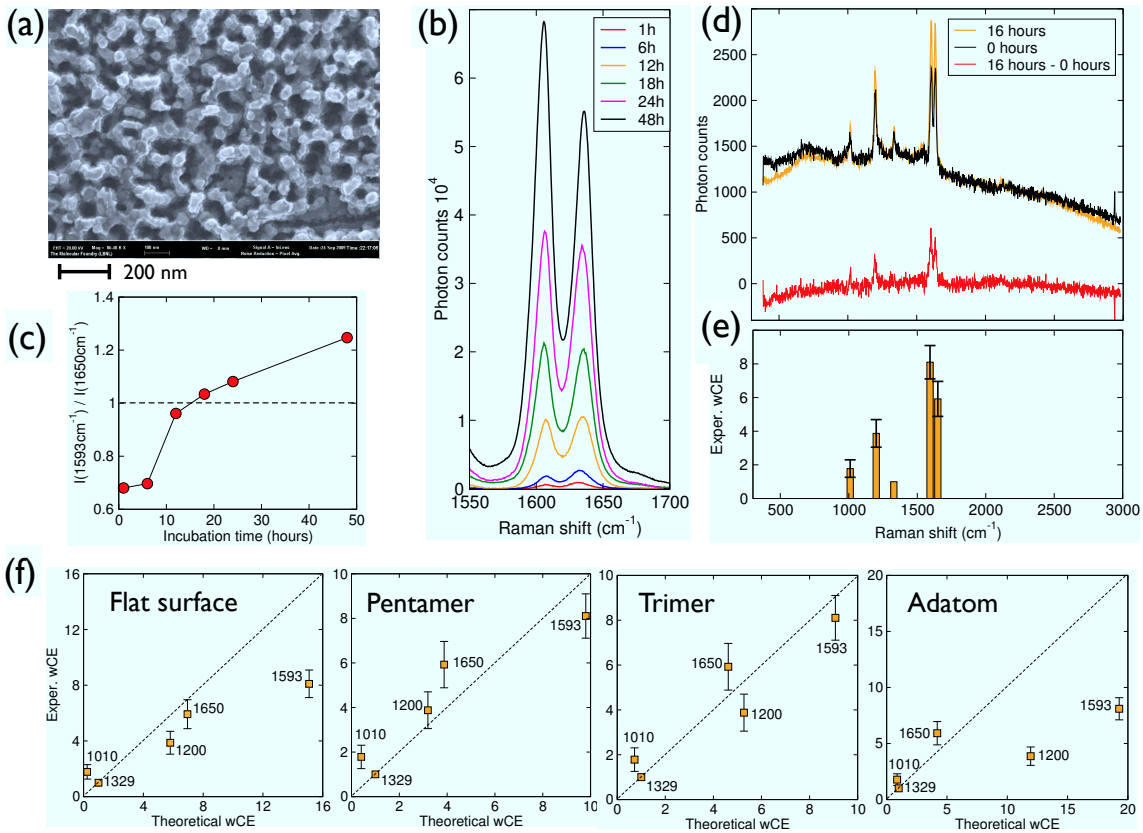


Figure 3: (a) SERS active SiGe substrate covered with Au used for measurements in this work. (b,c) Variation of intensities of the 1593 $cm^{-1}$ and 1650 $cm^{-1}$ peaks in SERS measurements of BPE as a function of substrates incubation time in BPE solution. (d) Two SERS spectra measured after 0 and 16 hours of incubation. By subtracting the two spectra, we extract the changes that are due to the chemical coupling, CE contribution. (e) By taking a sampling from several measurements, we estimate the standard error, and obtain averaged over all measurements CE effect. (f) The experimental difference from panel (e) compared directly with its theoretical counterpart. Both the binding Au atom coordination number and the theory-experiment agreement increase going from the "adatom" towards the "flat surface" geometry.

30 Å of vacuum. With the Au atoms in the bottom two layers of the slab fixed to their bulk values, the three upper layers are allowed to relax. While the 5-layered slab provides a good approximation for the macroscopic properties of Au surface, local atomic scale binding motifs of BPE to Au are not known. Accordingly, we consider several representive binding sites, differing mainly in the nearest-neighbor coordination number of the binding Au atom. For all sites considered, the in-plane slab lattice parameters are kept fixed to the bulk value calculated with PBE.[8] A 2x2x1 Monkhorst-Pack k-point mesh is used for calculations involving Au slab; the Γ point is used for finite system calculations. Following prior work, the static non-evanescent component of the Raman

tensor is constructed mode-by-mode using a finite-differences approach.[8]

Figure Figure 2(a) shows calculated Raman spectra of an isolated BPE molecule, and BPE adsorbed at four different binding sites. In all cases, BPE prefers to bind to undercoordinated gold atoms, and the highest binding energy is observed for the least coordinated binding site (adatom), with the binding energy monotonically decreasing for more coordinated geometries. As expected from prior work,[8] upon binding to Au, the BPE Raman spectra are altered in both relative peak heights and overall intensity. For the strongest Raman peak at 1593 $cm^{-1}$, calculated intensities are enhanced over isolated BPE by factors 13.4 , 40.4, 152.6, and 252.6 for the flat surface, pentamer, trimer, and adatom sites, respectively. Similarly, for the 1650 $cm^{-1}$ peak, the enhancements are 6.1, 14.8, 77.1, and 100.2. Evidently, independent of the binding site, the 1650 $cm^{-1}$ mode is enhanced less than the 1593 $cm^{-1}$ mode. As in previous works, the contributions to the Raman intensity can be rationalized with a two-state model, relating the changes in Raman spectra on binding to energy level alignment and enhancement of electron-phonon coupling associated with the interface.[8,9,17] In case of BPE, the lowest unoccupied molecular orbital ( LUMO) is the frontier state closest to the metal Fermi level, $E_F$, (see Figure S2) and the overall enhancement of Raman signal becomes stronger for smaller $(E_F - E_{LUMO})$. Of all binding sites considered, the adatom has the largest binding energy, smallest $E_F - E_{LUMO}$ difference (see Figure S2), and the largest Raman intensity enhancement. On the other hand, the flat surface binding site exhibits the least coupling between the molecule and the surface, and results in the least enhancement. A detailed picture rationalizing our DFT calculations in terms of the two-state model is given in Figure S2 of the Supplemental Information.

In all cases, our calculations show that binding inverts the intensity ratio of the 1593 $cm^{-1}$ and 1650 $cm^{-1}$ peaks. The 1593 $cm^{-1}$ vibrational mode clearly exhibits a stronger chemical coupling to the metal. In the language of the two-state model, the 1593 $cm^{-1}$ mode has a larger deformation potential,[8] therefore it is enhanced more than the 1650 $cm^{-1}$ mode. Thus, the relative strength of these peaks depends on whether the molecule is bound or not. From this observation, we conclude that the experimental variations in the 1593/1650 intensity ratio depend on the fraction of BPE

molecules bound to the substrate.

Based on the above discussion we find that the incubation time is the relevant parameter that we need to explore. New samples are prepared using the same Au-coated SiGe substrates as described above and shown in Fig. Figure 3(a). Substrates are incubated in the same container with BPE solution, and taken for measurements one at a time, starting at only a few minutes of incubation and continuing for two days. The 1593 $cm^{-1}$ and 1650 $cm^{-1}$ peaks in Fig. Figure 3(b) show a gradual change of their relative intensities; see also Fig. Figure 3(c). Our calculations (described above) suggest that the portion of chemically bound molecules contributing to the total SERS signal grows as the incubation time increases. The calculations also suggest that the peak inversion is a robust signature of binding, and does not depend significantly on the details of the binding site. The slow binding that we observe suggests that BPE molecules may initially compete with various impurities for binding sites; additionaly, van der Waals interactions could favor physisorption over direct chemical binding to the substrate.

The measurements at different incubation times provide a new, direct method of extracting the CE contribution to SERS spectra. Assuming the differences in intensity ratio between the short and long incubation times are due to CE, if we take the difference between spectra at different incubation times, we can extract the CE from the data. Figure Figure 3(d) shows two SERS spectra, measured after one minute and 16 hours of incubation, respectively, and the difference between the two spectra. Five measurements are taken at both times, yielding 25 combinations of zero and 16 hour measurements. This sampling provides a measure of the standard error for the data shown in Fig. Figure 3(e). The enhancement between factors of 2 and 8 is normalized by the least enhanced peak at 1326 $cm^{-1}$, following previous work.[8] We note that the estimated enhancements are only relative, not absolute values, which is due to the uncertainty in the absolute enhancement of our reference mode at 1326 $cm^{-1}$. If the reference mode had no chemical enhancement, then we could report absolute values of CE.

Because of the low concentration of BPE in solution, all molecules are on top of or very close to the surface, and experience essentially equivalent EM enhancements. We partition the Raman

cross section for a vibrational mode $n$ of a bound molecule as $\sigma^n_{Adsorbed} = \sigma^n_{Solution} + \sigma^n_{Interface}$, where $\sigma_{Solution}$ is the Raman cross section of an isolated gas-phase molecule, and $\sigma_{Interface}$ is the contribution from the molecule-metal binding. The chemical enhancement for vibrational mode $n$ is then defined as

$$CE^n = \frac{\sigma^n_{Adsorbed}}{\sigma^n_{Solution}} \tag{1}$$

Assuming all molecules are bound, we have previously shown that it is possible to extract CE from the experiment.[8] In that case, for $N_T$ molecules that bind close to hot spots, i.e. experience the EM ehnancement, the cross section will be $\Omega^n = EM\left\{N_T\sigma^n_{Adsorbed}\right\}$, where we suppress experimental setup factors, like intensity and polarization, for the purpose of this analysis. $EM$ is a constant after the plasmon dispersion correction[25,26] , as shown in Fig. Figure 1e. Similarly, for the solution Raman measurements $\tilde{\Omega}^n = N_{Solution}\sigma^n_{Solution}$, where $N_{Solution}$ is unknown. The total enhancement in this case can be expressed as

$$\frac{\Omega^n}{\tilde{\Omega}^n} = \frac{EM\left\{N_T\sigma^n_{Adsorbed}\right\}}{N_{Solution}\sigma^n_{Solution}} = \frac{N_T}{N_{Solution}} EM\cdot CE^n, \tag{2}$$

where $\frac{N_T}{N_{Solution}}$ is unknown. Normalizing Eq.2 with another vibrational mode $t$ removes $\frac{N_T}{N_{Solution}}$, resulting in a relative chemical enhancement. From the analysis of the deformation (shown in SI, Figure S2), some vibrational modes have negligible CE, i.e. $CE^t \approx 1$. If $CE^t = 1$ the ratio with mode $t$ leads us to the chemical enhancement

$$\frac{\Omega^n}{\tilde{\Omega}^n} \Big/ \frac{\Omega^t}{\tilde{\Omega}^t} = CE^n \tag{3}$$

We note that this approach is insufficient for BPE, where only a fraction of molecules are bound to the gold surface at any given time. In this case, the SERS cross section can be expressed as $\Omega^n = EM\left\{N_B\sigma^n_{Adsorbed} + N_{UB}\sigma^n_{Solution}\right\}$, with $N_B$ and $N_{UB}$ presenting the number of bound and unbound molecules, respectively. Using Eq.1 and $N_{UB} = N_T - N_B$, we can rewrite $\Omega^n = EM\sigma^n_{Solution}\left\{N_B\cdot CE^n + N_T - N_B\right\}$. We assume that $N_T$ is the same for all samples, which is

supported by an observation that the SERS peak of the least chemically enhanced mode at 1326 $cm^{-1}$ does not depend on the incubation time. If we also assume that samples with the shortest incubation time have no bound molecules, the corresponding "unbound" cross section can be written as $\tilde{\Omega}^n = EM\sigma^n_{Solution} \cdot N_T$. Subtracting spectra from samples with shorter and longer incubation time, as shown in Fig. Figure 3d, removes the total number of molecules, $N_T$, from the problem, $\Omega^n - \tilde{\Omega}^n = EM \cdot \sigma^n_{Solution} \cdot N_B(CE^n - 1)$. Normalizing this difference by the least enhanced mode $t$, we obtain the ratio

$$wCE^n = \frac{\Omega^n - \tilde{\Omega}^n}{\Omega^t - \tilde{\Omega}^t} = \frac{\sigma^n_{Solution}(CE^n - 1)}{\sigma^t_{Solution}(CE^t - 1)} \tag{4}$$

where we introduced $wCE^n$ as a "weighted CE" for mode $n$, whereby we have removed the efect of unbound molecules. It can be further simplified to $\frac{(CE^n-1)}{(CE^t-1)}$, as $\sigma^n_{Solution}$ and $\sigma^t_{Solution}$ are known, but for the purpose of this work, *wCE* can be directly evaluated from our DFT data, leading to a straightforward comparison of the experiment and theory. The experimental values of *wCE* are plotted in Fig. Figure 3(e).

Figure Figure 3(f) compares *wCE* values extracted from the experiment against the *wCEs* calculated for different binding sites . Interestingly, agreement with experiment is best for binding sites with equilibrium BPE geometries somewhat tilted relative to the surface normal. Tilting, along with CE, can also affect relative intensities in SERS spectra, although, in our case, to a significantly lesser extent than binding (see Figure S7 in SI). We note that while the adatom site has the largest binding energy for BPE, on a rough Au surface, adatoms inevitably aggregate to form structures like steps and islands, due to additional energy gains associated with higher coordination (see SI for direct calculation). Flat surfaces, on the other hand, result in a very low binding energy for BPE. Thus, the probability of BPE binding sites is determined by both binding energy and availability at given temperature. Our comparison to experiments ( Fig. Figure 3(f)) indicates that BPE on rough SERS substrates mostly binds to gold atoms which are more coordinated than adatoms, such as edges of islands or steps, with molecules exhibiting a modest, 30-40 degrees, tilt with respect to the surface normal. However, independently of the BPE tilt angle, the 1593 and 1650 $cm^{-1}$ peak reversal is a robust signature of chemical binding.

In summary, we have used chemical contributions in SERS to probe surface chemistry in detail for a specific analyte, BPE. First-principles calculations of static Raman intensities capture a significant part of the relative "chemical enhancement", which is confirmed by the agreement with the experimental data, and by rationalizing DFT calculations with a simple two-state model, where we discuss CE in terms of interfacial electronic structure and electron-phonon coupling. Using our understanding of relative CE, we have explained discrepancies in reported SERS data for BPE in terms of the relative number of bound molecules, and their variation from experiment to experiment. Our work paves the way for more elaborate uses of SERS for probing surface chemistry, ranging from surface catalysis to single molecule junctions.

## Acknowledgement

We thank M. Moskovits, G. Haran and R. P. Van Duyne for discussions, as well as our colleagues at Molecular Foundry and UC Berkeley. This work was supported by the AFOSR/DARPA Project BAA07-61 "SERS S&T Fundamentals" under contract FA9550-08-1-0257, and the Molecular Foundry through the Office of Science, Office of Basic Energy Sciences, of the U.S. Department of Energy under Contract No. DE-AC02-05CH11231. Computational resources were provided by DOE (LBNL Lawrencium, NERSC Franklin) and DOD (HPCMP ARL MJM).

## Supporting Information Available

The supplementary information contains additional data that is used to support the analysis of this work. This material is available free of charge via the Internet at `http://pubs.acs.org`.

## References

(1) Fleischman, M.; Hendra, P. J.; McQuillan, A. Raman spectra of pyridine at a silver electrode. *Chem. Phys. Lett.* **1974**, *26*, 163.

(2) Jeanmaire, D. L.; Duyne, R. P. V. Surface Raman spectroelectrochemistry: Part 1: Hete-

rocyclic, aromatic, and aliphatic amines adsorbed on the anodized silver electrode. *J. Electroanal. Chem.* **1977**, *84*, 1–20.

(3) Albrecht, M. G.; Creighton, J. A. Anomalously Intense Raman spectra of pyridine at a silver electrode. *J. Am. Chem. Soc.* **1977**, *99*, 5215.

(4) Moskovits, M. Surface-enhanced spectroscopy. *Rev. Mod. Phys.* **1985**, *57*, 783.

(5) Willets, K. A.; Duyne, R. P. V. Localized Surface Plasmon Resonance Spectroscopy and Sensing. *Annu. Rev. Phys. Chem.* **2007**, *58*, 267–297.

(6) Zheng, Y. B.; Payton, J. L.; Chung, C.-H.; Liu, R.; Cheunkar, S.; Pathem, B. K.; Yang, Y.; Jensen, L.; Weiss, P. S. Surface-Enhanced Raman spectroscopy to probe reversibly photoswitchable azobenzene in controlled nanoscale environments. *Nano Letters* **2011**, *11*, 3447–3452.

(7) Campion, A.; Kambhampati, P. Surface-enhanced Raman scattering. *Chem. Soc. Rev.* **1998**, *27*, 241.

(8) Zayak, A. T.; Hu, Y. S.; Choo, H.; Bokor, J.; Cabrini, S.; Schuck, P. J.; Neaton, J. B. Chemical Raman Enhancement of Organic Adsorbates on Metal Surfaces. *Phys. Rev. Lett.* **2011**, *106*, 083003.

(9) Jensen, L.; Aikens, C. M.; Schatz, G. C. Electronic structure methods for studying surface-enhanced Raman scattering. *Chem. Soc. Rev.* **2008**, *37*, 1061–1073.

(10) Lombardi, J. R.; Birke, R. L.; Lu, T.; Xu, J. Charge-transfer theory of surface-enhanced Raman spectroscopy. *J. Chem. Phys.* **1986**, *84*, 4174–4180.

(11) Heller, E. J.; Sundberg, R. L.; Tannor, D. Simple aspects of Raman scattering. *J. Phys. Chem.* **1982**, *86*, 1822–1833.

(12) Arenas, J. F.; Tocón, I. L.; Otero, J. C.; Marcos, J. I. Charge transfer processes in Surface-Enhanced Raman Scattering: Franck-Condon active vibrations of pyridine. *J. Phys. Chem.* **1996**, *100*, 9254–9261.

(13) Adrian, F. J. Charge transfer effect in surface-enhanced Raman scattering. *J. Chem. Phys.* **1982**, *77*, 5302.

(14) Persson, B. N. J.; Zhao, K.; Zhang, Z. Chemical contribution to Surface-Enhanced Raman Scattering. *Phys. Rev. Lett.* **2006**, *96*, 207401.

(15) Lombardi, J. R.; Birke, R. L. A Unified approach to Surface-Enhanced Raman Spectroscopy. *J. Phys. Chem. C* **2008**, *112*, 5605–5617.

(16) Lombardi, J. R.; Birke, R. L. The theory of surface-enhanced Raman scattering. *J. Chem. Phys.* **2012**, *136*, 144704.

(17) Morton, S. M.; Jensen, L. Understanding the Molecule-Surface chemical coupling in SERS. *J. Am. Chem. Soc.* **2009**, *131*, 4090.

(18) Kim, A.; Ou, F. S.; Ohlberg, D. A. A.; Hu, M.; Williams, R. S.; Li, Z. Study of molecular trapping inside gold nanofinger arrays on Surface-Enhanced Raman Substrates. *J. Am. Chem. Soc.* **2011**, *133*, 8234.

(19) Freeman, R. G.; Grabar, K. C.; Allison, K. J.; Bright, R. M.; Davis, J. A.; Guthrie, A. P.; Hommer, M. B.; Jackson, M. A.; Smith, P. C.; Walter, D. G.; Natan, M. J. Self-Assembled Metal Colloid Monolayers: An Approach to SERS substrates. *Science* **1995**, *267*, 1629–1632.

(20) Sun, G.; Grundmeier, G. Surface-Enhanced Raman Spectroscopy of the growth of ultra-thin organosilicon plasma polymers on nanoporous Ag/$SiO_2$-bilayer films. *Thin Solid Films* **2006**, *515*, 1266–1274.

(21) Hu, Y. S.; Jeon, J.; Seok, T. J.; Lee, S.; Hafner, J. H.; Drezek, R. A.; Choo, H. Enhanced

Raman Scattering from Nanoparticle-Decorated Nanocone Substrates: A Practical Approach to Harness In-Plane Excitation. *ACS Nano* **2010**, *4*, 5721–5730.

(22) He, L.; Natan, M. J.; Keating, C. D. Surface-Enhanced Raman Scattering: A Structure-Specific Detection Method for Capillary Electrophoresis. *Anal. Chem.* **2000**, *72*, 5348–5355.

(23) Liu, Y. J.; Zhang, Z. Y.; Zhao, Q.; Zhao, Y. P. Revisiting the separation dependent surface enhanced scattering. *Appl. Phys. Lett.* **2008**, *93*, 173106.

(24) Abell, J. L.; Driskell, J. D.; Dluhy, R. A.; Tripp, R. A.; Zhao, Y.-P. Fabrication and characterization of a multiwell array SERS chip with biological applications. *Biosensors and Bioelectronics* **2009**, *24*, 3663–3670.

(25) Buchanan, S.; Ru, E. C. L.; Etchegoin, P. G. Plasmon-dispersion corrections and constraints for surface selection rules of single molecule SERS spectra. *Phys. Chem. Chem. Phys.* **2009**, *11*, 7406–7411.

(26) Saikin, S. K.; Chu, Y.; Rappoport, D.; Crozier, K. B.; Aspuru-Guzik, A. Separation of Electromagnetic and Chemical Contributions to Surface-Enhanced Raman Spectra on Nanoengineered Plasmonic Substrates. *J. Phys. Chem. Lett.* **2010**, *1*, 2740–2746.

(27) Perdew, J. P.; Burke, K.; Ernzerhof, M. Generalized Gradient Approximation Made Simple. *Phys. Rev. Lett.* **1996**, *77*, 3865.

(28) Kresse, G.; Furthmüller, J. Efficient iterative schemes for ab initio total-energy calculations using a plane-wave basis set. *Phys. Rev. B* **1996**, *54*, 11169.

## DISCLAIMER



DE-AC02-05CH11231